2010 IEEE International Conference on Robotics and Automation
Anchorage Convention District
May 3-8, 2010, Anchorage, Alaska, USA

Analysis of Earthworm-like Robotic Locomotion on Compliant Surfaces

David Zarrouk[1], Inna Sharf[2], Moshe Shoham[3]

Abstract—**An inherent characteristic of biological vessels and tissues is that they exhibit significant compliance or flexibility, both in the normal and tangential directions. The latter in particular is atypical of standard engineering materials and presents additional challenges for designing robotic mechanisms for navigation inside biological vessels by crawling on the tissue. Several studies aimed at designing and building such robots have been carried out but little was done on analyzing the interactions between the robots and their flexible environment. In this study, we will analyze the interaction between earthworm robots and biological tissues where contact mechanics is the dominant factor. Specifically, the efficiency of locomotion of earthworm robots is derived as a function of the tangential flexibility, friction coefficients, number of cells in the robot and external forces.**

I. INTRODUCTION

Much of the interest in worm-like locomotion has been motivated by potential bio-medical applications of micro-robotic devices. Over the past decade, several research groups around the world expanded considerable efforts on developing robots for medical testing inside the gastrointestinal (GI) tract [1-5], and in respiratory system vessels [6], producing several robot designs and prototypes. However, little was done in terms of the analysis of the interaction between the robot and the biological tissue. Dario et al. considered a range of possible locomotion strategies for the GI tract and developed a number of robot prototypes [7-10]. Several pneumatic devices exploiting the *inchworm* extend-clamp principle of locomotion were proposed and tested in-vitro and in-vivo. The use of shape memory alloys for robot actuation was also investigated by Kim et al. 2005 [12] who developed and tested a capsule-like device with clamping and releasing mechanism. Significant advances in robot development for endoscopic applications have also been made by Chi and Yan 2003 [13] and Wang and Yan 2007 [14] who adopted earthworm-like locomotion for their prototypes. Very recently, a fully wireless (both for power and communication) earthworm-like flexible prototype was constructed.

Several publications to date have presented the analysis of locomotion efficiency (η) for inchworm-like robots [1,8,9] and earthworm robots [14,16]. The efficiency itself is usually stated as the ratio of the effective advance $L_{effective}$ in a cycle divided by the stroke L_s.

$$\eta = \frac{L_{effective}}{L_s} \tag{1}$$

The aim of the analysis is to evaluate the efficiency and critical stroke (minimum stroke that allows forward motion) in terms of the mechanical and material properties of the tissue. However, the locomotion efficiency is always defined for a single-stroke device, or in other words, by considering a two-segment robot only.

Our focus in this paper is on the analysis of locomotion efficiency of worm-like robotic devices in flexible environments for a device comprised of an *arbitrary* number of segments or cells n (also referred to in literature as units, cells and modules). In line with the literature review presented above, we consider the earthworm-robot which relies on frictional interaction between the device and vessel surfaces to enable locomotion.

Differently from the locomotion efficiency analysis presented to date in the literature, we derive analytical expressions for locomotion efficiency as a function of the number of cells n in the device. Our interest is to determine how locomotion efficiency of an earthworm-robot is affected by the number of cells, friction coefficients, contact forces and external forces (tether, weight or biological), and more specifically, if improvements in mechanical efficiency can be accrued by changing these parameters. In addition, our analysis is based on the use of *contact theory* to determine the critical stroke, which in turn implies that the interaction between the robot and the environment is viewed as a local phenomenon (local to the vicinity of the contact). Our analysis may be applicable to the intestinal environment, but is more relevant to other biological vessels, for example blood vessels, urinary tracts and respiratory system vessels. Finally, the analysis also illustrates a methodology for determining the locomotion efficiency in flexible environments which can be adopted to other types of locomotion then those considered in the paper.

II. SYSTEM DEFINITION

A. General description of worm-robots

We consider an n-module worm robot, driven by n-1 'axial' actuators which allow for extension and retraction of the modules, as shown in Fig. 1. We assume that the robot contacts the environment through the module surfaces only that is, at most n distinct and discrete locations, where the

[1] PhD candidate, Faculty of Mechanical Engineering, Technion-Israel Institute of Technology, Haifa, Israel (zadavid@tx.technion.ac.il)
[2] Department of Mechanical Engineering, McGill University, Montreal, Canada (inna.sharf@mcgill.ca)
[3] Faculty of Mechanical Engineering, Technion-Israel Institute of Technology, Haifa, Israel (shoham@tx.technion.ac.il)

friction forces are generated depending on whether the particular module is sliding or sticking.

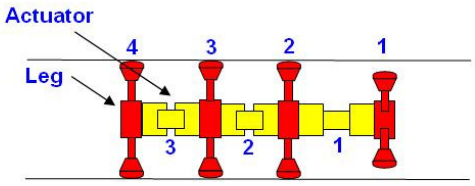

Fig 1. General wormlike robot

The worm robot advances by extending and contracting its axial actuators to move individual modules, typically one at a time. During the motion, the module can be completely unclamped from the surface or partially clamped. Thus, the motion of each module is characterized by three phases: unclamping (partial or full), translation (motion) and clamping to the surface again (full).

B. Friction and tangential compliance modelling

As already noted, friction is critical to enabling worm-like locomotion and it has to be considered in the locomotion efficiency analysis. For our purposes, we adopt the standard physical model of friction, the Coulomb model which gives an explicit definition for the force of friction, F_f as a function of the friction coefficient μ and the normal force F_n, during sliding as:

$$F_f = \mu F_n \tag{2}$$

In the present context, the normal force in the above is either the clamping or the unclamping force exerted by the robot modules on the environment. Our analysis also allows the coefficient of friction to vary between the directions of sliding (forward and backward), as well as between the clamped (μ_{fc} , μ_{bc}) and unclamped states (μ_{fu} , μ_{bu}) of the modules. The latter is representative of the situation when clamping is achieved by the deployment of setae (as is the case in the biological earthworms) or suction.

If there is no sliding at the contact, we assume that the force of friction is smaller than the sliding limit defined by (2) and is determined by the equilibrium of the system. Thus, in the present analysis, we will not differentiate between coefficients of dynamic and static friction.

The second major *modeling* component of the locomotion efficiency analysis is the model of tangential compliance which is coupled to the model of friction through the friction force. Differently from the previous analyses, the locomotion efficiencies developed in this manuscript are based on the *contact* model of tangential compliance, as opposed to the *structural* model.

The tangential compliance model of the environment connects the tangential force F_t (friction in our case) to the local tangential deformation of the surface δ. In the general analysis of Section III, we allow a general force-displacement relationship in the tangential direction, which we write as:

$$F_t = F_t(\delta) \tag{3}$$

We will also make use of the inverse of relation (3):

$$\delta(F_t) = F_t^{-1}\left(F_t(\delta)\right) \tag{4}$$

An important value of δ frequently used in our analysis is the maximum deflection which corresponds to the onset of sliding; it is evaluated with (5) and (6) for the backward and forward directions, respectively:

$$\delta_b = F_t^{-1}(-\mu_b F_n) \tag{5}$$

$$\delta_f = F_t^{-1}(\mu_f F_n) \tag{6}$$

C. Two-cell Earthworm Example

To illustrate the basic problem of loss of efficiency when a worm robot moves along a compliant environment, we consider one cycle of motion for a two-cell earthworm, moving in a straight compliant environment, under the application of a resisting force F_{ext} . Our specific goal is to determine the decrease in motion which results from the tangential compliance of the surface, over the complete cycle of motion. In evaluating the loss of stroke in this particular example, we will assume that no sliding takes place at the clamped cell of the robot and the force-deflection relation defining the tangential compliance is linear, in particular:

$$F_t = -k_t \delta \tag{7}$$

where k_t is the stiffness of the surface. The locomotion cycle of our two-module earthworm can be presented, accordingly, in two main stages, as illustrated in Fig. 2 for the case with the resisting force. As already mentioned, during the cycle, each cell executes three distinct phases: unclamping from the wall, motion and clamping to the wall.

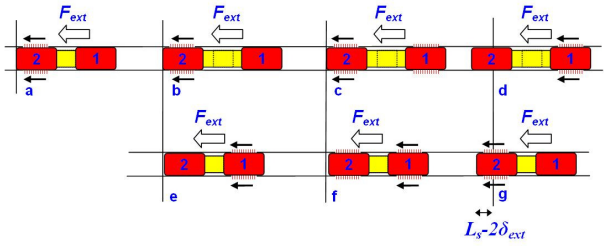

Fig 2 Two-cell earthworm advancing under the influence of a resisting force

Locomotion cycle of a two-cell earthworm as illustrated in Fig. 2. Starting with the initial configuration where the back cell (cell 2) is clamped and the fore cell (cell 1) is free (Fig. 2a), so that $\delta^{(2)} = \delta_{ext} = F_{ext} / k_t$:

Stage 1 Robot extends its body to advance the fore cell by L_s; fore cell clamps; back cell unclamps at which point $\delta^{(1)} = \delta_{ext}$. The robot moves backwards by δ_{ext} in this stage.

Stage 2 Robot retracts its body to advance the back cell by L_s; back cell clamps; fore cell unclamps at which point $\delta^{(2)} = \delta_{ext}$. The robot moves backwards by δ_{ext} in this stage.

At the end of the cycle, the robot has effectively advanced through $L_s - 2\delta_{ext}$ and therefore, the stroke loss is $2\delta_{ext} = 2F_{ext} / k_t$.

The locomotion efficiency defined as the ratio of the effective advance divided by the theoretical advance is therefore:

$$\eta = \frac{effective\ advance}{theoretical\ adavnce} = \frac{L_s - 2\delta_{ext}}{L_s} = 1 - \frac{2\delta_{ext}}{L_s} \qquad (8)$$

III. ANALYSIS OF WORM LOCOMOTION

We now develop an analytical formulation for the locomotion analysis of an *n*-module worm robot subject to an external force (Fig. 3). First, we state the basic conditions for the robot equilibrium, for its engagement with the wall as a whole, and for sticking to the wall of all individual modules. Then, the general motion analysis is presented for each of the three phases of the module (unclamping, motion and clamping).

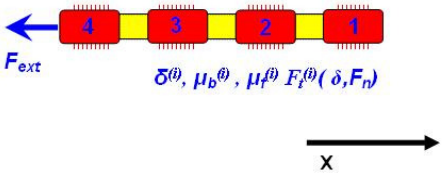

Fig 3. General worm under the influence of a force

A. Force conditions on worm robot

In quasistatic motion assumed in our analysis, the robot is in equilibrium so that the sum of all forces on the robot is zero. In the *x*-direction, the force equation is:

$$\sum F_t^{(i)}\left(\delta^{(i)}\right) + F_{ext} = 0 \qquad (9)$$

where summation is implied to be over *n* modules unless specified otherwise. The condition for robot engagement with the wall is stated in (10) and it defines the maximum external force that the robot can resist without the *whole* system sliding.

$$\left|F_{ext}\right| \le \sum \mu^{(i)} F_n^{(i)} \qquad (10)$$

However, partial sliding, that is, sliding at some of the modules can still occur under (10), while the robot as a whole remains engaged with the wall. We can also determine the condition required to prevent sliding at all of the modules. Thus, consider a worm robot, initially unloaded and an external force is applied to it. In this case, the robot will displace through a distance *r* during which some of the cells may slide even though the whole robot may remain engaged. To ensure that no sliding occurs at any of the cells, the displacement *r* must satisfy the following inequality:

$$r \le \min\left(\delta_{\max}^{(i)}\right) = \min\left(F_t^{(i)-1}\left(\mu^{(i)} F_n^{(i)}\right)\right) \qquad (11)$$

where δ_{max} is the maximum deflection under a specific cell that does not allow sliding; it is equal to δ_f and δ_b for forward and backward motions, respectively. The corresponding maximum external force allowed to ensure that no sliding happens between any of the modules and the wall is:

$$\left|F_{ext}\right| \le \sum F_t^{(i)}\left(\min\left(F_t^{(i)-1}\left(\mu^{(i)} F_n^{(i)}\right)\right)\right) \qquad (12)$$

B. Force and tangential deflection analysis for a single cell

Before we tackle the general motion analysis, it is useful to illustrate the effects on the tangential deflection of a single cell.

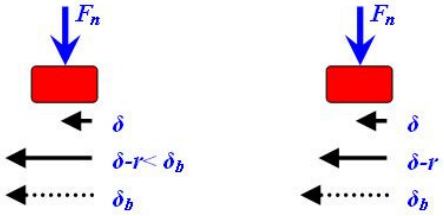

Fig 4. Value of tangential deflection when the cell is shifted by a distance *r*

Consider a cell already deflected through $\delta^{(i)}$, moved through a specified distance *r*. The final deflection of the cell will depend on whether the maximum deflection limit of this particular cell has been reached and we will determine it using an operator ⟦ ⟧ as:

$$\left[\!\left[\delta^{(i)} - r\right]\!\right] = \min\left(\delta^{(i)} - r, F_t^{(i)-1}\left(\mu\ F_n^{(i)}\right)\right) = \delta_{\max}^{(i)} \qquad (13)$$

Thus, as illustrated in Fig. 4, the final deflection is either $\delta^{(i)} - r$ if there is no sliding or $\delta_{\max}^{(i)}$ when sliding occurs.

C. General motion analysis

We now combine our understanding of the basic principles discussed in Sections A and B to carry out the locomotion analysis for the worm robot. In particular, the analysis makes use of the fact that at the end of any phase in the robot cycle, the worm robot must remain in equilibrium and any backward displacement that occurs during a particular phase must be applied to the whole system, that is, the robot is treated as a single rigid body. As described earlier, the worm robot cycle involves advancing all of its cells sequentially, one at a time, with each cell experiencing unclamping, moving and clamping. Each of the three phases may cause a change in the deflection under the cells of the robot and therefore it is convenient to analyze each phase separately. In all cases, the results are presented for the case when the first cell of the robot is moved (see Fig. 5), after

which we give a summary of how to apply the procedure to complete the full cycle of worm motion to determine the loss of stroke for the cycle.

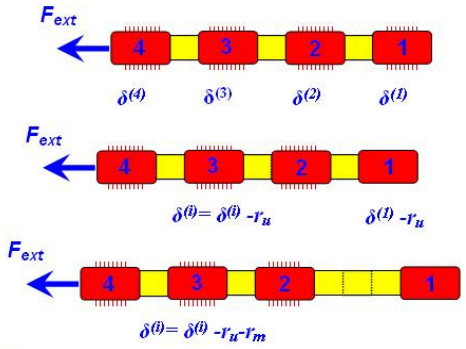

Fig 5. Deflection under the cells of an earthworm while moving cell 1

Unclamping phase: if the robot changes the friction coefficient (from μ_{fc} and μ_{bc} to μ_{fu} and μ_{bu} respectively) sliding may happen if

$$F_t^{(i)}\left(\delta^{(i)}\right) > \mu_{bu}^{(i)} F_n^{(i)} \tag{14}$$

In this case, the robot will slide and r_u can be calculated from

$$\sum_{i\neq 1} F_t^{(i)}\left(\left[\!\left[\delta^{(i)} - r_{u,sl}\right]\!\right]\right) + \mu_{bu}^{(1)} F_n^{(1)} + F_{ext} = 0 \tag{15}$$

Motion phase: In the motion phase, the body of the robot will move back by a distance r_m which can be calculated from

$$\sum_{i\neq 1} F_t^{(i)}\left(\left[\!\left[\delta^{(i)} - r_u - r_m\right]\!\right]\right) - \mu_{fu}^{(1)} F_n^{(1)} + F_{ext} = 0 \tag{16}$$

Clamping phase: In the clamping stage, there is no additional backward motion due to increase in the coefficient of friction since the robot is already static.

Completing the cycle: Having determined the backward displacements of the robot in the unclamping and motion phases of a single module (r_u, and r_m), these are added up to get the corresponding total backward displacement r. In order to determine the displacement of the robot after a full cycle, this analysis must be repeated for each cell, as the cells are moved through the actuator stroke, and updating the position and absolute tangential deflection of each cell accordingly. The final net advancement of the robot is then computed from:

$$L_{cycle} = L_s - \sum r^{(i)} \tag{17}$$

The locomotion efficiency is thus calculated with:

$$\eta = 1 - \frac{\sum r^{(i)}}{L_s} \tag{18}$$

IV. SPECIAL CASES ANALYSIS

A. Locomotion of worm-robot with identical cells

In this section, we specialize the development of locomotion efficiency to a worm with identical cells. This means they share the same friction coefficients (μ_f, μ_b), and the same model of tangential compliance $F_t(\delta)$. The 'uniform' worm was chosen first, because it is representative of real robot systems and second, because it allows us to gain better insight into the locomotion losses of the worm.

The first interesting characteristic of such a worm is that after a few cycles, the distribution of deflections under the cells reaches an arithmetic sequence. A specific number of cells moved last, which we denote here by *m,* may reach the maximum deflection δ_b and slide. Table I presents the progression of displacements under all cells for a five-cell worm robot for the complete cycle of motion.

TABLE I
TANGENTIAL DEFLECTION UNDER THE CELLS OF THE WORM

Leg number	5	4	3	2	1
Start	δ_f	$\delta_f - r$	$\delta_f - 2r$	δ_b	δ_b
After advancing cell 1	$\delta_f - r$	$\delta_f - 2r$	δ_b	δ_b	δ_f
After advancing cell 2	$\delta_f - 2r$	δ_b	δ_b	δ_f	$\delta_f - r$
After advancing cell 3	δ_b	δ_b	δ_f	$\delta_f - r$	$\delta_f - 2r$
After advancing cell 4	δ_b	δ_f	$\delta_f - r$	$\delta_f - 2r$	δ_b
After advancing cell 5	δ_f	$\delta_f - r$	$\delta_f - 2r$	δ_b	δ_b

Thus, for example, when the robot makes the first step, cell 1 moves forwards and the tangential deflection underneath it changes from δ_b to δ_f; cell 2 slides during the whole motion while cell 3 sticks until its deflection reaches δ_b and then starts sliding. The deflections of cells 4 and 5 decrease by the increment of the arithmetic sequence *r*.

B. Locomotion Analysis of worm-robot with linear tangential compliance.

We now specialize our locomotion efficiency analysis further by restricting the model of tangential compliance to be linear, that is:

$$F_t = \begin{cases} -k_t\delta & \delta_b \le \delta \le \delta_f \\ -\mu_f F_n & \delta \ge \delta_f \\ \mu_b F_n & \delta \le \delta_b \end{cases} \qquad \begin{bmatrix} \delta_f = \mu_f F_n / k_t \\ \delta_b = -\mu_b F_n / k_t \end{bmatrix} \tag{19}$$

and the tangential deflections for the "start" phase (see Table I) are given by:

$$\delta^{(i)} = \begin{cases} \delta_f - r(n-i) & i \le n-m \\ -\delta_b & i > n-m \end{cases} \tag{20}$$

Therefore, the force equilibrium equation (9) simplifies to:

$$-m\delta_b - \left(\frac{n-m}{2}\right)\left(\delta^{(n)} + \delta^{(m+1)}\right) + F_{ext}/k_t = 0 \tag{21}$$

or

$$m\delta_b + \left(\frac{n-m}{2}\right)\left(2\delta_f - r\left(n-m-1\right)\right) - \delta_{ext} = 0 \qquad (22)$$

where $\delta_{ext} = F_{ext} / k_t$ is the tangential deflection due to the external force. Solving (22) for the increment r yields:

$$r = \frac{2\left(\delta_f - \frac{\delta_{ext} - m\delta_b}{n-m}\right)}{n-m-1} \qquad (23)$$

Next we calculate the number of cells that will slide, i.e., the value of m. Since we know that cell m+1 did not slide in the previous phase (cell 3 at "start" in Table I), then:

$$\delta^{(m+1)} > -\delta_{\max} \qquad (24)$$

Inserting (20) into (24) yields:

$$\delta_f - r\left(n-m-1\right) > \delta_b \qquad (25)$$

and substituting for the increment r from Eq. (23) we get:

$$\delta_f - \delta_b > \frac{2\left(\delta_f\left(n-m\right) - \delta_{ext} + m\delta_b\right)}{n-m} \qquad (26)$$

The above can be solved for m to get:

$$m > \frac{-2\delta_{ext} + n\left(\delta_f + \delta_b\right)}{\delta_f - \delta_b} \qquad (27)$$

Thus, the number of cells sliding is the smallest integer m which satisfies the inequality (27). The resultant net advancement in every cycle can now be evaluated by subtracting from the stroke the loss of stroke to give:

$$L_{cycle} = L_s - n \cdot r = L_s - \frac{2n}{n-m-1}\left(\delta_f - \frac{\delta_{ext} - m\delta_b}{n-m}\right) \qquad (28)$$

V. SIMULATION RESULTS AND COMPARISON TO ANALYSIS

A numerical simulation of earthworm robot locomotion was developed and results compared to the theoretical predictions of loss of motion. In the numerical simulation, the stroke of the robot is divided into many small steps during which the positions of the cells as well as the tangential deflections are calculated using Eqs.

(9) and (21). The purpose of the simulations is first to validate the analytical predictions of the locomotion efficiency, as well as the results in Table I and Eqs. (17), (23) and (28). The second objective is to demonstrate the actual possible loss of efficiency by using realistic parameters for the environment and the robot.

We consider the motion of an earthworm comprised of four modules moving on a surface inclined at an angle α=0.1 rad as shown in Fig. 6 In terms of efficiency of locomotion, this example is identical to a robot moving under the influence of a tether force equivalent to approximately 10% of its weight.

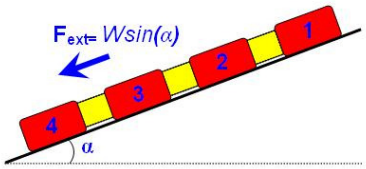

Fig 6. An earthworm advancing a slope

The value of the tangential flexibility k_t is taken from our own experiments on a fresh aorta of a bull, (k_t=79.3mN/mm). The robot is assumed to weigh 200g, its stroke L_s=10mm, μ_f=0.1 and μ_b=0.2. Fig. 7 displays the advance of the first cell of the earthworm calculated from the simulated motion of the first cell vs. the theoretical expectation of the position, as per Eq. (28). It shows a clear agreement between them, taking into account that the analytical prediction reflects the overall advance of the robot in a cycle and not the incremental advances as is the case in simulation.

The simulated position of the cell clearly exhibits the cyclical motion and furthermore, one can discern in each cycle a single motion forward and three motions backwards. A more comprehensive view is presented in Fig. 8 where we display a zoom into the position of the first cell during one of the cycles (cycle 4). Here, we annotate point A which corresponds to the beginning of the motion of the first cell; subsequently, at point B the first cell slows down because one of the cells started sliding backwards (in this case, cell 3). Continuing, at point C the motion speeds up because the first cell starts sliding in the forward direction and the body of the robot is no longer moving backwards. Point D shows the end of the stroke of the first cell, after which the first cell displaces back (three times) through a distance r (the increment of the sequence) due to the movement of the three other cells. The distance travelled by the robot in this cycle is 4.96mm (r=5.04mm), which for the stroke of 10mm yields the efficiency of locomotion of only 49.6%.

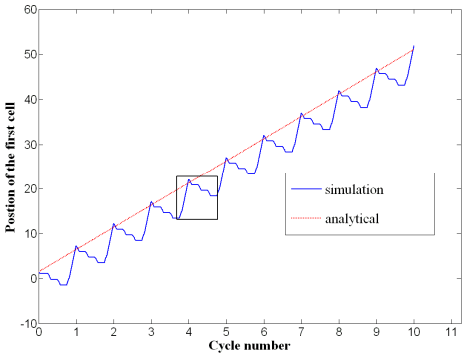

Fig 7.Numerical simulation vs. analytical solution of the earthworm with resisting force

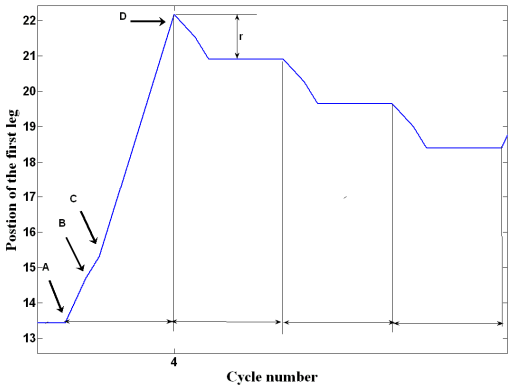

Fig 8. Position of a cell during a full cycle

VI. CONCLUSIONS

The research described in the present manuscript focused on the analysis of worm robotic locomotion in a flexible environment, motivated by the biomedical applications of worm robots. Differently from the previous analyses, we considered worm-like robots comprised of an arbitrary number of cells. Furthermore, the basic assumption used to derive the net motion in a cycle is that the environment is compliant only in the vicinity of contact points with the robot and hence, contact analysis could be used. We began our presentation with the general formulation of the physics of locomotion for earthworm robots with different cell properties and then, proceeded to consider special cases of robots with similar cells and linear model of tangential compliance. The latter simplification allowed us to obtain explicit results for locomotion efficiency as a function of the tangential compliance, the number of cells, friction coefficients and external forces. We anticipate these results to be useful both for the analysis and the design of worm robots.

It was shown that unlike what has been proposed in some previous studies, the tangential flexibility has an *additive* effect on the motion loss and that for accurate analysis, the previous deflections of the robot cells must be remembered and changes accumulated. Our analysis also revealed that the tangential deflections under the cells form an arithmetic sequence. This behavior causes an unequal load distribution on the different cells causing some to slide, thereby further decreasing the efficiency of motion.

A numerical simulation of worm locomotion was developed and its results found to be in excellent agreement with our analysis of locomotion. The model of tangential compliance was based on the contact properties of an aorta of a bull and the resulting locomotion efficiency was reduced by 50%. The authors' future work will be devoted to the analysis of the behavior of worms on non-linear elastic surfaces and where structural deformations are large.

REFERENCES

[1] P. Dario, P. Ciarletta, A. Menciassi, and B. Kim, "Modeling and experimental validation of the locomotion of endoscopic robots in the colon," *International Journal of Robotics Research*, 23(4-5), pp. 549-556, 2004.

[2] A. Menciassi, D. Accoto, S. Gorini, and P. Dario, "Development of a biomimetic miniature robotic crawler," *Autonomous Robots*, 21 (2), pp. 155-163, 2006.

[3] T. Nakamura, and T. Iwanaga, "Locomotion strategy for a peristaltic crawling robot in a 2-dimensional space," *Proceedings IEEE International Conference on Robotics and Automation*, art. no. 4543215, pp. 238-243, 2008.

[4] K. Wang, G. Yan, P. Jiang and D. Ye, "A wireless robotic endoscope for gastrointestine," *IEEE Transactions on Robotics,* 24 (1), pp. 206-210, 2008.

[5] K. Wang, G. Yan, G. Ma and D. Ye, "An earthworm-like robotic endoscope system for human intestine: Design, analysis, and experiment," *Annals of Biomedical Engineering,* 37 (1), pp. 210-221, 2009.

[6] L. Z. Yu, G. Z. Yan, and X. R Wang, "A flexible micro-robot system for direct monitoring in human trachea ," *Jiqiren/Robot* 28 (3), pp. 269-274, 2006.

[7] I. Kassim, L. Phee, W. S. Ng, G. Feng, P. Dario and C.A. Mosse, "Locomotion techniques for robotic colonoscopy ," *IEEE Engineering in Medicine and Biology Magazine*, 25 (3), pp. 49-56, 2006.

[8] L. Phee, A. Menciassi, S. Gorini, G. Pernorio, A. Arena, and P. Dario, "An innovative locomotion principle for minirobots moving in the gastrointestinal tract," *Proceedings IEEE International Conference on Robotics and Automation* (Cat. No.02CH37292), p 1125-30 vol.2, 2002.

[9] L. Phee, D. Accoto, A. Menciassi, C. Stefanini, M.C. Carrozza and P. Dario, "Analysis and development of locomotion devices for the gastrointestinal tract," *IEEE Transactions on Biomedical Engineering*, 49(6), pp. 613-616, 2002.

[10] L. Phee, A. Menciassi, D. Accoto, C. Stefanini, and P. Dario, "Analysis of robotic locomotion devices for the gastrointestinal tract," *Robotics Research, STAR 6*, pp. 467-483, 2003.

[11] A. Menciassi, S. Gorini, G. Pernorio, and P. Dario, "A SMA actuated artificial earthworm," *Proceedings IEEE International Conference on Robotics and Automation*, , pp. 3282-3287, 2004.

[12] B. Kim, S. Lee and J. Park, "Design and fabrication of a locomotive mechanism for capsule-type endoscopes using shape memory alloys (SMAs)," *IEEE/ASME Transactions on Mechatronics*, 10(1), pp. 77-86, 2005.

[13] D. Chi and G. Yan,. "From wired to wireless: a miniature robot for intestinal inspection," Journal of Medical Engineering & Technology, 27(2), pp. 71-76, 2003.

[14] K. Wang and G. Yan, "Micro robot prototype for colonoscopy and in vitro experiments," *Journal of Medical Engineering & Technology*, 31(1), pp. 24-28, 2007.

[15] W.D. Li, W. Guo, M.T. Li and Y.H. Zhu , "Design and test of a capsule type endoscope robot with novel locomotion principle," *9th International Conference on Control, Automation, Robotics and Vision* (IEEE Cat. No.06EX1361), p 6, 2006.

[16] J. Kwon, S. Park, J. Park, and B. Kim, "Evaluation of the critical stroke of an earthworm-like robot for capsule endoscopes," *Proceedings of the Institution of Mechanical Engineers, Part H* (*Journal of Engineering in Medicine*), 221(114), pp. 397-405, 2007.